

## Toll-Like Receptor 2 Enhances ZO-1–Associated Intestinal Epithelial Barrier Integrity Via Protein Kinase C

ELKE CARIO,\* GUIDO GERKEN,\* and DANIEL K. PODOLSKY†

\*Division of Gastroenterology and Hepatology, University Hospital of Essen, Essen, Germany; and †Gastrointestinal Unit, Massachusetts General Hospital, Center for the Study of Inflammatory Bowel Disease, Harvard Medical School, Boston, Massachusetts

**Background & Aims:** Protein kinase C (PKC) has been implicated in regulation of intestinal epithelial integrity in response to luminal bacteria. Intestinal epithelial cells (IECs) constitutively express Toll-like receptor (TLR)2, which contains multiple potential PKC binding sites. The aim of this study was to determine whether TLR2 may activate PKC in response to specific ligands, thus potentially modulating barrier function in IECs. **Methods:** TLR2 agonist (synthetic bacterial lipopeptide Pam<sub>3</sub>CysSK<sub>4</sub>, peptidoglycan)–induced activation of PKC-related signaling cascades were assessed by immunoprecipitation, Western blotting, immunofluorescence, and kinase assays—combined with functional transfection studies in the human model IEC lines HT-29 and Caco-2. Transepithelial electrical resistance characterized intestinal epithelial barrier function. **Results:** Stimulation with TLR2 ligands led to activation (phosphorylation, enzymatic activity, translocation) of specific PKC isoforms (PKC $\alpha$  and PKC $\delta$ ). Phosphorylation of PKC by TLR2 ligands was blocked specifically by transfection with a TLR2 deletion mutant. Ligand-induced activation of TLR2 greatly enhanced transepithelial resistance in IECs, which was prevented by pretreatment with PKC-selective antagonists. This effect correlated with apical tightening and sealing of tight junction (TJ)-associated ZO-1, which was mediated via PKC in response to TLR2 ligands, whereas morphologic changes of occludin, claudin-1, or actin cytoskeleton were not evident. Downstream the endogenous PKC substrate myristoylated alanine-rich C kinase substrate (MARCKS), but not transcriptional factor activator protein-1 (AP-1), was activated significantly on stimulation. **Conclusions:** The present study provides evidence that PKC is an essential component of the TLR2 signaling pathway with the physiologic consequence of directly enhancing intestinal epithelial integrity through translocation of ZO-1 on activation.

The intestinal epithelium constitutes an anatomic as well as immunologic barrier that forms a bipolar interface between the diverse populations of luminal microbes and immune cells of the underlying lamina propria. Barrier function is maintained by a complex

interplay of numerous proteins within the tight-junction (TJ) complex.<sup>1</sup> Biogenesis of TJ is regulated selectively by protein kinase C (PKC), and the TJ protein zonula occludens-1 (ZO-1) appears to be a specific target of PKC.<sup>2</sup>

Disruption of the sensitive equilibrium of TJs may be elicited by a number of pathogenic bacteria and proinflammatory cytokines, exacerbating and perpetuating intestinal inflammation in disease.<sup>3</sup> To counteract potential harmful effects of luminal toxins and to protect barrier homeostasis, intestinal epithelial cells (IECs) exhibit several defensive features, including production of intestinal trefoil peptides and mucins.<sup>4</sup> Commensals also may assist the host to confer intestinal epithelial barrier integrity.<sup>5,6</sup> However, the underlying mechanisms of these beneficial host-microbe interactions that may tighten the paracellular seal are largely unclear.

Toll-like receptors (TLRs) comprise a class of pattern-recognition receptors that specifically discriminate between self- and microbial non-self-based on the recognition of broadly conserved molecular patterns.<sup>7</sup> TLRs play a key role in microbial recognition, control of adaptive immune responses, and induction of antimicrobial effector pathways, leading to efficient elimination of host-threatening pathogens. We and others recently have shown that IECs express several TLRs, including TLR2 and TLR4, in vitro and in vivo.<sup>8–14</sup> As the frontline of the mucosal immune system, the intestinal epithelium constantly is exposed to large amounts of various TLR ligands that appear to coexist in the intestinal mucosa.<sup>15</sup> To maintain mucosal homeostasis, inflammatory re-

---

*Abbreviations used in this paper:* AP-1, activator protein-1; FITC, fluorescein isothiocyanate; IEC, intestinal epithelial cell; LPS, lipopolysaccharide; MARCKS, myristoylated alanine-rich C kinase substrate; PGN, peptidoglycan; PKC, protein kinase C; PMA, phorbol 12-myristate 13-acetate; TER, transepithelial resistance; TJ, tight junction; TLR, Toll-like receptor; TLR2DN, dominant-negative construct of Toll-like receptor 2; TLR4DN, dominant-negative construct of Toll-like receptor 4; ZO-1, zonula occludens-1.

© 2004 by the American Gastroenterological Association

0016-5085/04/\$30.00

doi:10.1053/j.gastro.2004.04.015

sponses are suppressed toward commensals, leading to the phenomenon of tolerance in the healthy gut. Decreased expression of TLRs and high levels of Tollip appear to correlate with inhibition of proinflammatory responses in the face of commensals.<sup>11,16,17</sup> However, lipopolysaccharide (LPS) may acutely elicit several proinflammatory responses in some IECs.<sup>8,18</sup> Cytokine-induced imbalance in inflammation also might lead to intestinal intolerance toward LPS by altering TLR4 expression and triggering exaggerated downstream events that promote disease.<sup>18,19</sup>

The PKC superfamily is known to consist of at least 11 isozymes with selective tissue distribution and cell localization as well as numerous activators and substrates, thus modulating a complex array of diverse cellular functions and immune responses. Based on their structure and cofactor regulation, PKC isoforms have been classified into 3 groups: conventional ( $\alpha$ ,  $\beta_I$ ,  $\beta_{II}$ ,  $\gamma$ ), novel ( $\delta$ ,  $\epsilon$ ,  $\eta$ ,  $\mu$ ,  $\theta$ ), and atypical ( $\zeta$ ,  $\iota/\lambda$ ). Differential mechanisms of PKC-isozyme regulation include phosphorylation, which modulates the active enzymatic site and subcellular trafficking.<sup>20,21</sup> In *Drosophila*, atypical PKC is required for stimulation of the Toll-signaling pathway, leading to activation of the nuclear factor  $\kappa$  B homologues Dif and Dorsal, controlling the transcriptional activity of the Drosomycin promoter.<sup>22</sup> Inhibition of various PKC isoforms using pseudosubstrate peptides or pharmacologic inhibitors are thought to impair LPS signaling in human dendritic cells<sup>23</sup> and murine macrophages.<sup>24</sup> Moreover, LPS-stimulated macrophages from PKC $\epsilon$   $-/-$  appear to be deficient in the induction of nitric oxide synthase, suggesting that PKC $\epsilon$  is an essential downstream target of LPS signaling.<sup>25</sup> However, a direct causal connection of PKC activation with the TLR-signaling pathway has not been established in the mammalian system so far.

It recently has been suggested that IECs remain broadly hyporesponsive to TLR2 ligands<sup>16</sup> and, so far, no functional role has been ascribed to TLR2 in IECs. Because TLR2 contains multiple potential PKC-binding sites, we speculated that specific isoforms of PKC might be activated in response to TLR2 ligands. To understand the specific biologic consequence of PKC activation via TLR2 in IECs, we analyzed PKC-induced signaling events and morphologic changes in response to bacterial ligands in this study.

## Materials and Methods

### Reagents and Antibodies

The synthetic lipopeptide Pam<sub>3</sub>Cys-SK<sub>4</sub> [PCSK]; lots #D06, G05, K05, F06, G06) was

obtained from EMC Microcollections GmbH (Tübingen, Germany) and were prepared as recommended by the manufacturer. In brief, Pam<sub>3</sub>CysSK<sub>4</sub> was dissolved in sterile (endotoxin < 0.005 EU/mL) H<sub>2</sub>O (ICN, Aurora, OH), thoroughly vortexed, stored in small aliquots for up to 8 weeks at  $-20^{\circ}\text{C}$ , and treated with ultrasonics before use. Peptidoglycan (PGN) from *Staphylococcus aureus* (lot #14427/1) was purchased from Fluka (Buchs, Switzerland) and dissolved in sterile Dulbecco's phosphate-buffered saline (PBS) without  $\text{Ca}^{2+}/\text{Mg}^{2+}$  (PAA Laboratories, Linz, Austria), thoroughly sonicated for 5 minutes on ice, and stored in small aliquots at  $-20^{\circ}\text{C}$ . Highly purified (99.9% free of DNA and protein) LPS from *Escherichia coli*, serotype R515 (lot #L11290) was obtained from Alexis Biochemicals (Grünberg, Germany). Rottlerin and Gö6976 were purchased from Merck Biosciences (Schwalbach, Germany). Phorbol 12-myristate 13-acetate (PMA) was obtained from Sigma-Aldrich (Taufkirchen, Germany).

Rabbit polyclonal antibodies to conventional PKC $\alpha$  (C-20), novel PKC $\delta$  (C-17),<sup>26</sup> and panPKC (H-300) were obtained from Santa Cruz Biotechnology (Santa Cruz, CA). Rabbit polyclonal antibodies to phospho-panPKC, phospho-PKC $\alpha/\beta_{II}$  (threonine 638/641), phospho-PKC $\delta/\theta$  (serine 643/676), and phospho-myristoylated alanine-rich C kinase substrate (MARCKS) (serine 152/156) were purchased from Cell Signaling Technology (Beverly, MA). As indicated by the manufacturer, phospho-panPKC antibody detects endogenous levels of PKC $\alpha$ ,  $\beta_I$ ,  $\beta_{II}$ ,  $\delta$ ,  $\epsilon$ ,  $\eta$ , and  $\theta$  isoforms only when phosphorylated at a carboxy-terminal residue homologous to serine 660 of PKC $\beta_{II}$  and does not detect PKC phosphorylated at other sites. Extracts of U937 cells treated with 0.2  $\mu\text{mol/L}$  PMA for 30 minutes were kindly provided by Cell Signaling Technology as proven positive control for phosphorylation of pan-PKC and PKC $\delta$ .<sup>27</sup> Mouse monoclonal antibodies to  $\beta$ -actin and flag-M2 were obtained from Sigma-Aldrich. Rabbit polyclonal antibodies to occludin and claudin-1 and mouse monoclonal to ZO-1 were purchased from Zymed (South San Francisco, CA). Horseradish-peroxidase-conjugated anti-rabbit and anti-mouse antibodies were purchased from Amersham Pharmacia Biotech (Freiburg, Germany). Fluorescein isothiocyanate (FITC)-conjugated goat anti-rabbit immunoglobulin (Ig)G antibody was purchased from Vector Laboratories (Burlingame, CA). FITC-conjugated goat anti-mouse IgG antibody was obtained from Jackson ImmunoResearch Laboratories (West Grove, PA). CY5-conjugated goat anti-rabbit IgG antibody was a gift from Dr. Jens Nürnberger (Division of Nephrology, University Hospital of Essen, Germany). Normal rabbit IgG (Santa Cruz) and mouse IgG (Ebioscience, San Diego, CA) were used as negative controls. All other reagents were obtained from Sigma-Aldrich unless otherwise specified.

### Cell Culture

Two different IEC lines, Caco-2 (#5-23) and HT-29 (#3-20), were obtained from the American Type Culture Collection (Manassas, VA) through LGC Promochem, Teddington, Middlesex, United Kingdom, (lot #1537739 [HTB-37])

and lot #1467609 [HTB-38], respectively) and kept in a humidified incubator at 37°C with 5% CO<sub>2</sub>. Caco-2 were maintained in high-glucose (4.5 g/L) Dulbecco's modified Eagle medium (PAA Laboratories), supplemented with 20% vol/vol non-heat-inactivated fetal calf serum (PAA Laboratories, endotoxin-free, lot #A01121-245), 100 U/mL penicillin, and 100 µg/mL streptomycin (PAA Laboratories). When cultured on semipermeable membranes, Caco-2 cells spontaneously differentiate into a highly functionalized epithelial barrier exhibiting similar structural and biochemical characteristics as mature enterocytes. HT-29 were maintained in glucose (3.0 g/L)-containing McCoy's 5A medium (Invitrogen, San Diego, CA), supplemented with 10% vol/vol non-heat-inactivated fetal calf serum, 100 U/mL penicillin, and 100 µg/mL streptomycin. In contrast to Caco-2 cells, HT-29 cells thus were kept undifferentiated with very low transepithelial resistance after reaching confluence.<sup>28</sup> When subconfluent, Caco-2 cells were passaged by gentle mechanical disruption and HT-29 cells by treatment with enzyme-free, Hanks'-based, cell dissociation buffer (Invitrogen). Media of Caco-2 and HT-29 cells was changed 2 and 3 times, respectively, per week.

### Western Blotting and Immunoprecipitation

Cells were subjected to last media change 24–36 hours before stimulation. After incubation with stimuli, cells were rinsed twice in cold PBS (without Ca<sup>2+</sup>/Mg<sup>2+</sup>) with 100 µmol/L Na<sub>3</sub>VO<sub>4</sub>, and then lysed in ice-cold lysis buffer (1% NP-40 [Pierce, Rockford, IL], 50 mmol/L NaCl, 20 mmol/L Tris-HCl, pH 7.4, 2 mmol/L ethylenediaminetetraacetic acid, containing 10 mmol/L NaF, 10 mmol/L dithiothreitol, 10 mmol/L Na<sub>3</sub>VO<sub>4</sub>, complete miniprotease inhibitor cocktail tablet [Roche, Mannheim, Germany], and 2 mmol/L phenylmethyl sulfonyl fluoride plus [Roche]). Lysates were centrifuged (12,000 × g, 15 min, at 4°C), and protein concentration in each supernatant was determined by colorimetric Bradford protein assay (Bio-Rad, Hercules, CA). For immunoprecipitation, the supernatants were precleared at 4°C overnight by adding 2.5 µg of anti-rabbit IgG and 100 µL protein A agarose (3% vol/vol; Amersham) and then incubated with primary antibody (1:200) and 100 µL of protein A agarose (3%) overnight at 4°C. Beads were washed 4 times with ice-cold lysis buffer and processed for further Western blotting. Proteins were heated in NuPAGE LDS sample buffer (Invitrogen) after addition of 1 mmol/L dithiothreitol (85°C, 2 min), subjected to sodium dodecyl sulfate–polyacrylamide gel (10-, 12-, or 15-well, 4%–12% Bis-Tris; Invitrogen) electrophoresis at 130 V, transferred onto a polyvinylidene difluoride membrane (Millipore, Eschborn, Germany) at 30 V, followed by blocking (Tris-buffered saline tween-20 with 5% nonfat dry milk or 1%–5% bovine serum albumin) for 1 hour at room temperature, washing with Tris-buffered saline tween-20 for 5 minutes 3 times, immunoblotting with primary antibody (1:500–1:1000 in 5% nonfat dry milk or 0.1%–5% bovine serum albumin) for overnight at 4°C, and then with horseradish-peroxidase–conjugated secondary antibody (1:8000 in 4%

nonfat dry milk in Tris-buffered saline tween-20) for 1 hour at room temperature. After washing with Tris-buffered saline tween-20 for 5 minutes 3 times, the membrane was developed with the enhanced chemiluminescence detection kit Renaissance (NEN Life Science, Boston, MA) and exposed for different time periods (10 s–20 min) to Kodak BioMax Light film (Kodak GmbH, Stuttgart, Germany) followed by manual processing (Adefo Chemie, Nürnberg, Germany) in a standardized way (developing, 10 s–2 min; rinsing, 30 s; fixation, 5 min; washing, 5–10 min). To confirm equal loading, immunoblots were stripped with 62.5 mmol/L Tris-HCl, pH 6.8, 2% sodium dodecyl sulfate, containing 100 mmol/L 2-ME at 50°C for 30 minutes and reprobbed with anti-β-actin (1:10,000) or anti-panPKC (1:500). Images of Western blots were acquired in a standardized way (800 dpi) using an Epson Perfection 1640SU-Photo scanner (Seiko Epson Corp., Nagano, Japan) and digitized with Adobe Photoshop 5.0LE (Adobe Systems, Inc., Palo Alto, CA). All experiments were repeated at least 3 times; representative results are shown for each experiment.

### In Vitro Kinase Assay

HT-29 monolayers, grown at 70% confluence on 100-mm tissue culture dishes, were stimulated and washed twice with cold PBS (without Ca<sup>2+</sup>/Mg<sup>2+</sup>) containing 100 µmol/L Na<sub>3</sub>VO<sub>4</sub>. Proteins were extracted by 10-minute incubation on ice with 750 µL of lysis buffer (1% NP-40, 50 mmol/L HEPES, pH 7.4, 100 mmol/L NaCl, 2 mmol/L ethylenediaminetetraacetic acid, 2 mmol/L ethylene glycol-bis(β-aminoethyl ether)-N,N,N',N'-tetraacetic acid, 50 mmol/L NaF, 1 mmol/L Na<sub>3</sub>VO<sub>4</sub>, 5 mmol/L β-glycerophosphate, and 2 mmol/L phenylmethyl sulfonyl fluoride). After centrifugation for 10 minutes at 12,000 × g at 4°C, and adjustment of protein concentrations, lysates (600 µL/sample) were incubated immediately with polyclonal antibodies against cPKCα (3 µg) or nPKCδ (3 µg) and protein-A Sepharose beads for overnight rotation at 4°C. After centrifugation for 10 minutes at 12,000 × g at 4°C, beads were washed twice with ice-cold lysis buffer, resuspended in 20 µL of prewarmed kinase buffer using a brightly colored, fluorescent PKC-specific peptide substrate (PepTag nonradioactive protein kinase C assay; Promega, Madison, WI), and incubated for 30 minutes at 30°C. Samples then were boiled for 10 minutes, vortexed, and centrifuged at 12,000 × g for 5 minutes at room temperature, followed by electrophoresis (100 V, 15 min) on a 0.8% agarose gel (50 mmol/L Tris-HCl, pH 8.0). Phosphorylation by PKC of the substrate alters the peptide's net charge from +1 to -1, thereby allowing the active and inactive versions of the substrate to be separated rapidly by electrophoresis and visualized under ultraviolet light. The PKC positive (active) and negative (inactive) controls were used as supplied by the manufacturer. All experiments were repeated at least 3 times; representative results are shown for each experiment.

### Confocal Immunofluorescence

Caco-2 cells were cultured on 4-well permanox slide-chambers (NalgeNunc, Naperville, IL) until differentiated

(unless otherwise indicated in the Results section), stimulated, and washed twice with PBS (without  $\text{Ca}^{2+}/\text{Mg}^{2+}$ ) at 37°C.

For assessment of protein kinase C isoform translocation, cells were fixed with fresh, ice-cold 4% paraformaldehyde containing 0.1% Triton X-100 for 60 minutes at 4°C followed by washing with ice-cold PBS. Cells were blocked with 1% goat serum (Vector) and 1% bovine serum albumin in PBS for 60 minutes at room temperature and incubated with primary antibody (cPKC $\alpha$  or nPKC $\delta$ ; 1:100) or normal rabbit IgG (equivalent dilution) as negative control (data not shown) in blocking buffer containing 0.1% Triton X-100 overnight at 4°C.

For assessment of TJ assembly and transfection efficiency, cells were fixed with methanol/acetone (50:50) for 5 minutes at -20°C, air-dried, and washed with TBST. Cells were blocked with normal goat serum (1:100 in PBS) for 60 minutes at room temperature and incubated with primary antibody (claudin-1, occludin, ZO-1, or flag-M2; 1:100) or normal rabbit/mouse IgG (equivalent dilution) as negative controls (data not shown) in PBS overnight at 4°C.

FITC-conjugated goat anti-rabbit, anti-mouse, and CY5-conjugated goat anti-rabbit IgG antibodies were used as secondary antibody (1:250 or 1:200, 60 min, room temperature). rhodamine- or Alexa Fluor647-conjugated phalloidin (1:40, Molecular Probes, Eugene, OR) were added to counterstain filamentous actin to mark cell boundaries (data not shown for all results). Samples were mounted (Vectashield mounting media with or without DAPI; Vector Laboratories) and assessed within the next 24 hours by using a laser-scanning confocal microscope (Plan-Apochromat 63 $\times$ /1.40 (oil) DIC objective, Zeiss Axiovert 100M-LSM 510; Carl Zeiss, Oberkochen, Germany). At least 5 individual sites of image capture were chosen randomly in areas of uniform monolayer thickness for each sample. To establish comparable conditions between individual cell monolayers, equivalent images of equal number of horizontal slices (1024  $\times$  1024 pixels) with the same vertical depth from apical tip to basal membrane between nonstimulated and stimulated monolayers (as indicated in the Results section) were acquired. Height of intestinal epithelial monolayers was used as an indirect marker of cell differentiation.<sup>14,29,30</sup> All images were captured under identical laser settings. Results were considered significant only if more than 70% of the scanned sections per field exhibited the observed effect. Single XY planes (parallel to cell monolayer) and reconstructed XZ/YZ planes (orthogonal to cell monolayer) were processed using standardized 2-color or monochannel settings (software LSM510 v3.2) and exported to Adobe Photoshop 5.0LE. All experiments were repeated at least 3 times; representative results are shown for each experiment.

### Assessment of Intestinal Epithelial Barrier Function

Transepithelial resistance (TER) was used as a measure of paracellular permeability and barrier function in confluent Caco-2 monolayers that were maintained on 6-well cellulose

transwell permeable inserts (BD Falcon, Franklin Lakes, NJ; 0.4- $\mu\text{mol/L}$  filter pore size, high density). Confluency of Caco-2 monolayers usually was reached within 5–10 days and cells were used for experiments 21–30 days after seeding. Twenty-four–36 hours before stimulation, cells were equilibrated with fresh medium with an apical and basolateral volume of each 2 mL. Each individual stimulation was performed in triplicate with matched negative controls on the same 6-well plate. For TER measurements, Millicell-ERS epithelial volt-ohm meter (Millipore) was used under standardized conditions with electrodes equivalently placed and washed with warm medium between each measurement. After subtraction of the media and filter resistance ( $\sim 145 \Omega$ ), TER values were adjusted for the filter surface (4.2  $\text{cm}^2$ ) and expressed as  $\Omega \cdot \text{cm}^2$ .

### Plasmids, Transfection, and Luciferase Assay

The flag-tagged dominant-negative TLR2 (TLR2DN) and dominant-negative TLR4 (TLR4DN) expression plasmids were kindly provided by Tularik Inc. (South San Francisco, CA) through Dr. Carsten J. Kirschning (Institute of Medical Microbiology, Immunology, and Hygiene, Technical University of Munich, Munich, Germany) and both were confirmed by sequencing (Sequencing Core Facility, Institute of Human Genetics, University Hospital of Essen) and restriction analysis. Mammalian TLRs contain a very divergent ligand-binding ectodomain and a highly conserved cytoplasmic signaling domain (Toll/interleukin-1R domain). Mutagenesis and functional studies previously have shown that human TLRs interact via Toll/interleukin-1R domain with downstream signaling partners to transmit immune responses.<sup>31</sup> Therefore, TLR2DN and TLR4DN were generated by deletion of this intracellular signaling domain with truncation of the carboxyl-terminal portion of the wild-type molecule, implying that overexpression of these nonsignaling proteins impairs activation of downstream signaling pathways in response to specific ectodomain-binding ligands, as described earlier.<sup>32–34</sup> pCMV-(cytomegalovirus)-Flag1 (Sigma) was used as appropriate control vector. pAP1(PMA)-TA-Luciferase Vector<sup>35</sup> was obtained from BD Clontech and pSV- $\beta$ -Galactosidase Control Vector was obtained from Promega. Plasmids were prepared using the EndoFree Maxi plasmid kit (Qiagen, Hilden, Germany). HT-29 or Caco-2 cells were transfected transiently overnight (Lipofectamine 2000; Invitrogen), according to the manufacturer's instructions, with optimal concentrations of the plasmids (as specified later) in serum-free Optimum I media (Invitrogen), which was changed to full media the following day after transfection. Cells were stimulated 2 days after transfection and subsequently assayed as indicated in the Results section.

For assessment of PKC phosphorylation (as described earlier), HT-29 cells ( $1\text{--}5 \times 10^5/\text{mL}$ ) were transfected with TLR2DN or control vector at a final concentration of 1  $\mu\text{g}/\text{well}$  the following day after seeding. Caco-2 cells grown to 100% confluency on inserts of 6-well plates were transfected

with TLR2DN, TLR4DN, or control vector at final concentrations of 0.1 ng–0.4  $\mu\text{g}/\text{chamber}$  (as indicated in the Results section). To normalize for individual transfections, protein concentrations were equalized<sup>36</sup> and confirmed by reprobing for constitutively expressed  $\beta$ -actin (data not shown) and pan-PKC.

For measurements of TER (as described earlier), Caco-2 monolayers fully differentiated onto inserts were transfected with TLR2DN, TLR4DN, or control vector 14–21 days after seeding at a final concentration of 0.4  $\mu\text{g}/\text{chamber}$  in triplicate. Directly after TER measurements, cells were fixed (as described earlier) and filters were cut out. Transfection efficiency subsequently was visualized by immunostaining with anti-Flag M2 monoclonal, as described earlier. The number of nuclei (DAPI) of at least 5 identical field sizes per sample were counted and the percentage of green fluorescing cells was determined.<sup>37</sup> Transiently transfected cells presented optimal and consistent expression of flag-tagged deletion mutants under pCMV-promoter at day 2 posttransfection. The transfection efficiency was estimated at an approximate range from 80%–90% (data not shown).

For activator protein-1 (AP-1) luciferase assays, Caco-2 cells grown onto 6-well plates at 90% confluency were cotransfected with 0.5  $\mu\text{g}/\text{well}$  of pAP1(PMA)-TA-Luc and 0.1  $\mu\text{g}/\text{well}$  of pSV  $\beta$ -galactosidase in triplicate. Cell lysates were assayed for firefly luciferase activity using the Luciferase Reporter Assay System (Promega) in a luminometer (TD20/20; Turner Biosystems, Sunnyvale, CA) under standardized conditions. Data were normalized to  $\beta$ -galactosidase activity (as an internal control for transfection efficiency), measured by the luminescent  $\beta$ -galactosidase detection kit II (BD Clontech). All individual experiments were performed in triplicate.

### Statistical Analysis

Data are expressed as mean  $\pm$  SD of 3 or more independent experiments. Differences between means were evaluated by using the heteroscedastic, 2-sided *t* test (Microsoft Excel; Microsoft, Redmond, WA) where appropriate. *P* values of  $<0.05$  were considered significant.

## Results

### TLR2 Ligands Rapidly Phosphorylate PKC Complex

As previously shown, IECs constitutively express TLR2.<sup>8</sup> A synthetic, protein-free, and sterile preparation of a TLR2-specific lipopeptide,<sup>38</sup> Pam<sub>3</sub>CysSK4, was used to study TLR2 stimulation to exclude effects of potential contaminants<sup>39</sup> that might contribute to PKC activation. Results were confirmed using phenol-extracted PGN from *S. aureus*, as a second TLR2-binding ligand.<sup>40</sup> To exclude that PGN-responsive NOD2/CARD15<sup>41,42</sup> may be involved in PKC signaling, Caco-2 cells, which do not express NOD2,<sup>43</sup> were used in all experiments and re-

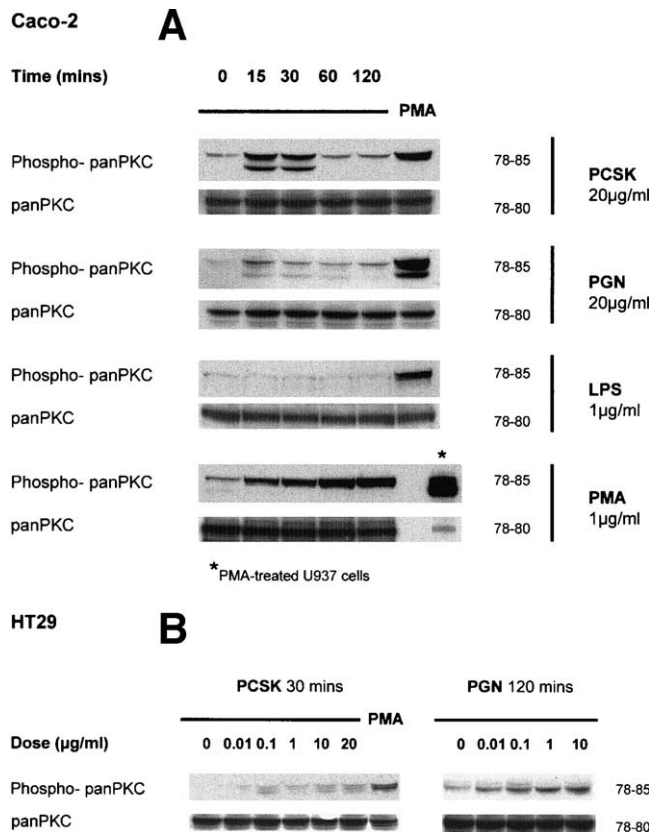


**Figure 1.** TLR2 ligands induce phosphorylation of PKC complex in a time- and concentration-dependent manner. (A) Caco-2 monolayers were treated with Pam<sub>3</sub>CysSK4 (20  $\mu\text{g}/\text{mL}$ ), PGN (20  $\mu\text{g}/\text{mL}$ ), LPS (1  $\mu\text{g}/\text{mL}$ ), or PMA (1  $\mu\text{g}/\text{mL}$ ) for the indicated time periods (15–120 min). (B) HT-29 monolayers were treated with different doses (10 ng–20  $\mu\text{g}/\text{mL}$ ) of TLR2 ligands, Pam<sub>3</sub>CysSK4 or PGN, for the indicated time periods (30 or 120 min, respectively). Cell lysates were immunoblotted and probed with anti-phospho-panPKC antibody, as described in the Materials and Methods section. To confirm equal loading and to exclude effects on total PKC expression, blots were reprobed with either anti-panPKC (nonphosphorylated) or anti- $\beta$ -actin (data not shown). \*PMA-treated U937 cells.

sults were compared with those in the NOD2-expressing cell line HT-29.

Stimulation of the 2 different IEC lines (HT-29, Caco-2) with the 2 TLR2 ligands resulted in significant phosphorylation of PKC complex in a time- and concentration-dependent manner (representative blots are shown in Figure 1A, B). Both Pam<sub>3</sub>CysSK4 and PGN induced significant phosphorylation of PKC complex after 15 minutes of stimulation. Pam<sub>3</sub>CysSK4-induced activation returned to resting levels after 60 minutes, whereas PGN-induced activation lasted up to 120 minutes (Figure 1A). It recently has been shown that the specific activity of lipopeptides varies with environmental conditions (e.g., oxidation, de-esterification,<sup>44</sup> and micelle formation [according to the manufacturer]), which may have caused the short and variable duration of

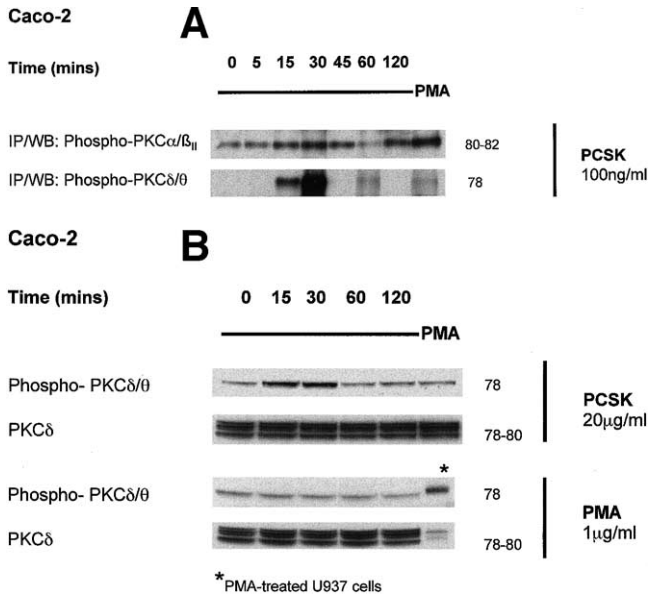


**Figure 2.** TLR2 ligands specifically phosphorylate conventional PKCα/β<sub>II</sub> and novel PKCδ/θ. (A) Caco-2 monolayers were treated with low-dose Pam<sub>3</sub>CysSK4 (100 ng/mL) for various time periods (5–120 min) and subjected to immunoprecipitation followed by immunoblotting with isoform-specific antibodies to phosphorylated PKCα/β<sub>II</sub> or phosphorylated PKCδ/θ. PMA (500 ng/mL) was used as presumed positive control (60-min stimulation). (B) Caco-2 monolayers were treated with Pam<sub>3</sub>CysSK4 (20 μg/mL) or PMA (1 μg/mL) for indicated time periods (15–120 min). Cell lysates were immunoblotted and probed with anti-phospho-PKCδ/θ antibody, as described in the Materials and Methods section. To confirm equal loading, blots were re-probed with anti-PKCδ (nonphosphorylated). \*PMA-treated U937 cells.

biologic activity of Pam<sub>3</sub>CysSK4 compared with PGN in our experiments. In the absence of TLR2 stimulation, minimal baseline PKC activity was detectable, presumably reflecting primarily physical stress. Concentration response experiments indicated that 10 ng/mL of either Pam<sub>3</sub>CysSK4 or PGN was sufficient to cause significant phosphorylation of PKC complex after 30 minutes or 120 minutes, respectively (Figure 1B). In contrast, stimulation with the TLR4 ligand LPS did not lead to sufficient phosphorylation of PKC complex at any time point tested (Figure 1A). PMA broadly activates PKC complex in U937 cells,<sup>27</sup> detecting several isoforms as part of the PKC complex between 78 and 85 kilodaltons (Figure 1A). However, in comparison with TLR2 ligands, our results show that PMA strongly stimulated phosphorylation of other isoforms of PKC complex with different kinetics in IEC.

**TLR2 Ligands Specifically Activate 2 Isoforms: PKCα and PKCδ**

To identify the involved isoforms of PKC complex activated in response to Pam<sub>3</sub>CysSK4, immunoprecipitation studies were performed with specific antibod-

ies to individual phosphorylated PKC isoforms (Figure 2A). Addition of small amounts of Pam<sub>3</sub>CysSK4 (100 ng/mL) led to significant time-dependent phosphorylation of conventional PKCα/β<sub>II</sub> and novel PKCδ/θ, both reaching maximum peaks after 30 minutes and thus confirming initial kinetic results with the antibody against the broad range of phosphorylated PKC isoforms. Phosphorylation of both PKC isozyme groups already was evident after 15 minutes of stimulation. By using this sensitive method, phosphorylation of PKCα/β<sub>II</sub> was detectable for up to 120 minutes, whereas phosphorylation of PKCδ/θ no longer was evident after 45 minutes. The positive control (PMA-treated U937 cell extracts) supplied by the manufacturer confirmed specificity of the antibody detecting phosphorylated PKCδ/θ at 78 kilodaltons (Figure 2B). In contrast to Pam<sub>3</sub>CysSK4, PMA did not lead to significant phosphorylation of PKCδ/θ between 15 to 120 minutes of stimulation in IECs (Figure 2A, B), implying selective activation of specific PKC isoforms by different ligands in different cell lines.

Specific ligand-induced activation of PKC isoforms is not only reflected by the status of phosphorylation but also by the level of enzymatic activity and evidence of subcellular translocation.<sup>45</sup> To confirm that Pam<sub>3</sub>CysSK4 indeed activates specific PKC isoforms, 2 additional methodologic approaches were included in our studies: *in vitro* kinase assay for enzymatic activity and confocal immunohistochemistry for subcellular localization of PKC isoforms. *In vitro* kinase assays confirmed that phosphorylation initiated enzymatic activation of the 2 PKC isoforms α and δ in response to Pam<sub>3</sub>CysSK4. As shown in Figure 3, Pam<sub>3</sub>CysSK4 led to significant enzymatic activation of PKCα and δ after 60 minutes of stimulation, which already was evident after 30 minutes (data not shown). Consistent with the preceding finding in Figure 2, stimulation with PMA (1 μg/mL, 60 min) induced significant enzymatic activation of PKCα, but only minimally of PKCδ.

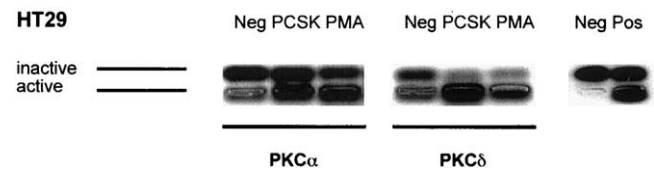


**Figure 3.** The TLR2 ligand Pam<sub>3</sub>CysSK4 induces enzymatic activation of conventional PKCα and novel PKCδ. HT-29 monolayers were treated with Pam<sub>3</sub>CysSK4 (20 μg/mL) or PMA (1 μg/mL) for 60 minutes. Cell lysates were immunoprecipitated with isoform-specific antibodies and subjected to *in vitro* kinase reaction with the PepTag nonradioactive PKC assay for assessment of PKCα and PKCδ activity, as described in the Materials and Methods section. Negative and positive controls represent inactive and active PKC included in the assay.

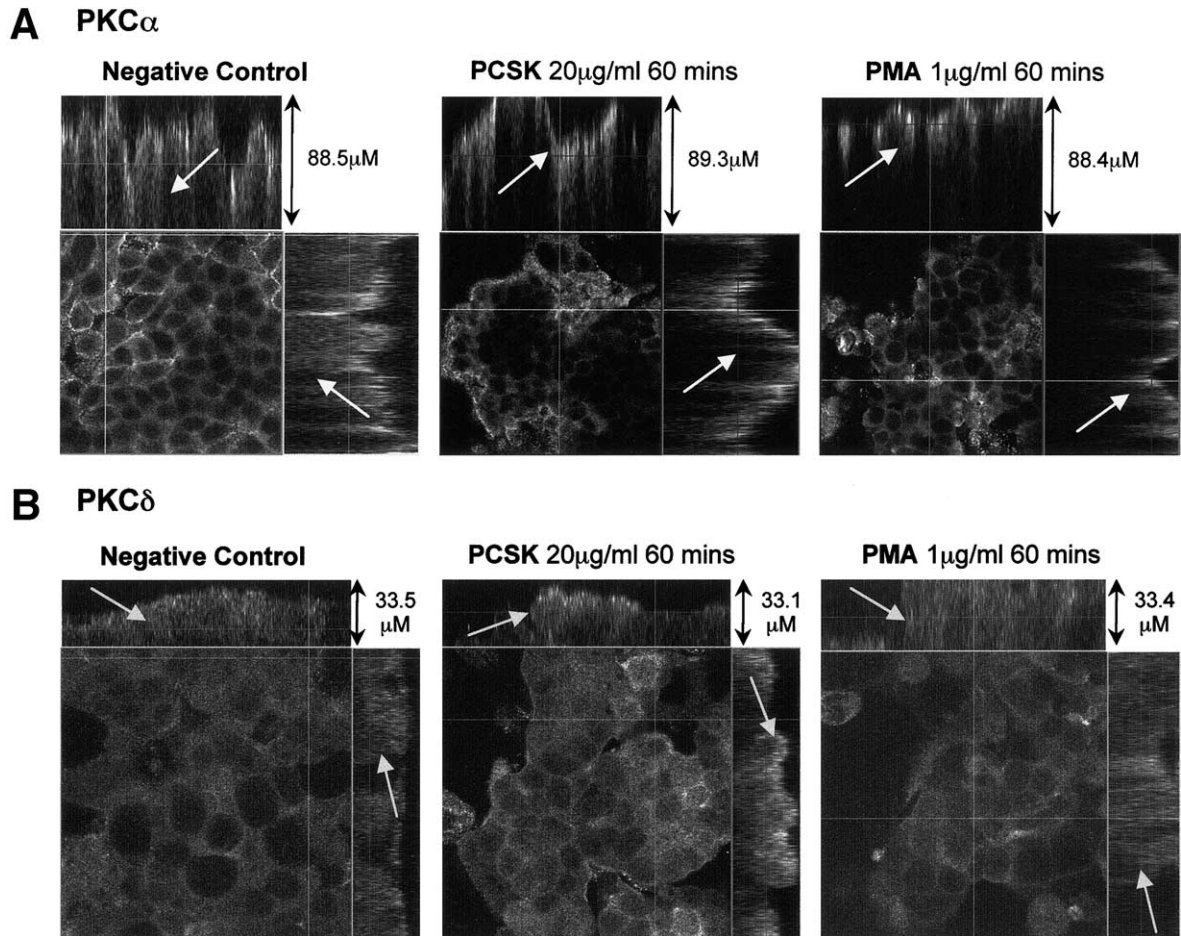


**Figure 4.** The TLR2 ligand Pam<sub>3</sub>CysSK4 induced apical translocation of PKC $\alpha$  and PKC $\delta$ . Caco-2 cells were grown on chamber slides until confluent and treated with Pam<sub>3</sub>CysSK4 (20  $\mu$ g/mL) or PMA (1  $\mu$ g/mL) for 60 minutes and translocation of (A) PKC $\alpha$  or (B) PKC $\delta$  isoforms was visualized by immunostaining with isoform-specific nonphosphorylated antibodies followed by FITC-conjugated secondary antibody and confocal microscopy, as described in the Materials and Methods section. Negative controls were left untreated. Cells were counterstained with phalloidin to outline cell boundaries (data not shown). Vertical height of cell monolayer was used as an indirect marker of the state of cell differentiation: (A) differentiated, (B) nondifferentiated.<sup>14,29,30</sup> Representative images of XZ, YZ, and XY stacks are shown (monochannel: FITC). *Grey lines* indicate location of XZ/YZ-stacks in XY-stack, as well as location of XY-stack in XZ/YZ-stacks, respectively. *White arrow* indicates localization of PKC-isoform. (63 $\times$ /1.4 oil, scan zoom 1.0, total scanning depth of 15–30 Z-stacks per monolayer is indicated per individual image.)

In parallel, translocation of both isoforms, PKC $\alpha$  (Figure 4A) and PKC $\delta$  (Figure 4B), from cytosolic compartments to apical membrane and subapical cytoplasmic domains was apparent at 30 minutes (data not shown) and maximal at 60 minutes after addition of Pam<sub>3</sub>CysSK4 in Caco-2 monolayers—regardless of whether they were differentiated (Figure 4A) or nondifferentiated (Figure 4B). In nontreated monolayers (negative control), both PKC isoforms were dispersed in the cytosolic compartments without distinct apical or basolateral preference. In contrast, PMA induced translocation of PKC $\alpha$ , but not of PKC $\delta$ , in Caco-2 monolayers.

As shown in Figure 1A, the TLR4 ligand LPS did not induce significant phosphorylation of PKC complex. Neither enzymatic activation nor translocation of PKC

isoforms in response to LPS was detected (data not shown).

#### Activation of PKC Is Mediated Directly Via TLR2

To confirm that TLR2 ligand-induced PKC activation was mediated directly via TLR2, Caco-2 or HT-29 cells were transfected transiently with deletion mutants of TLR2, TLR4, or appropriate control vector and incubated in the presence or absence of Pam<sub>3</sub>CysSK4 or PGN (Figure 5). Although it has been shown that PMA-induced myeloid cell differentiation correlates with up-regulation of TLR2 messenger RNA and TLR4 messenger RNA expression after long-term stimulation,<sup>46</sup> PMA is not known to bind directly or activate

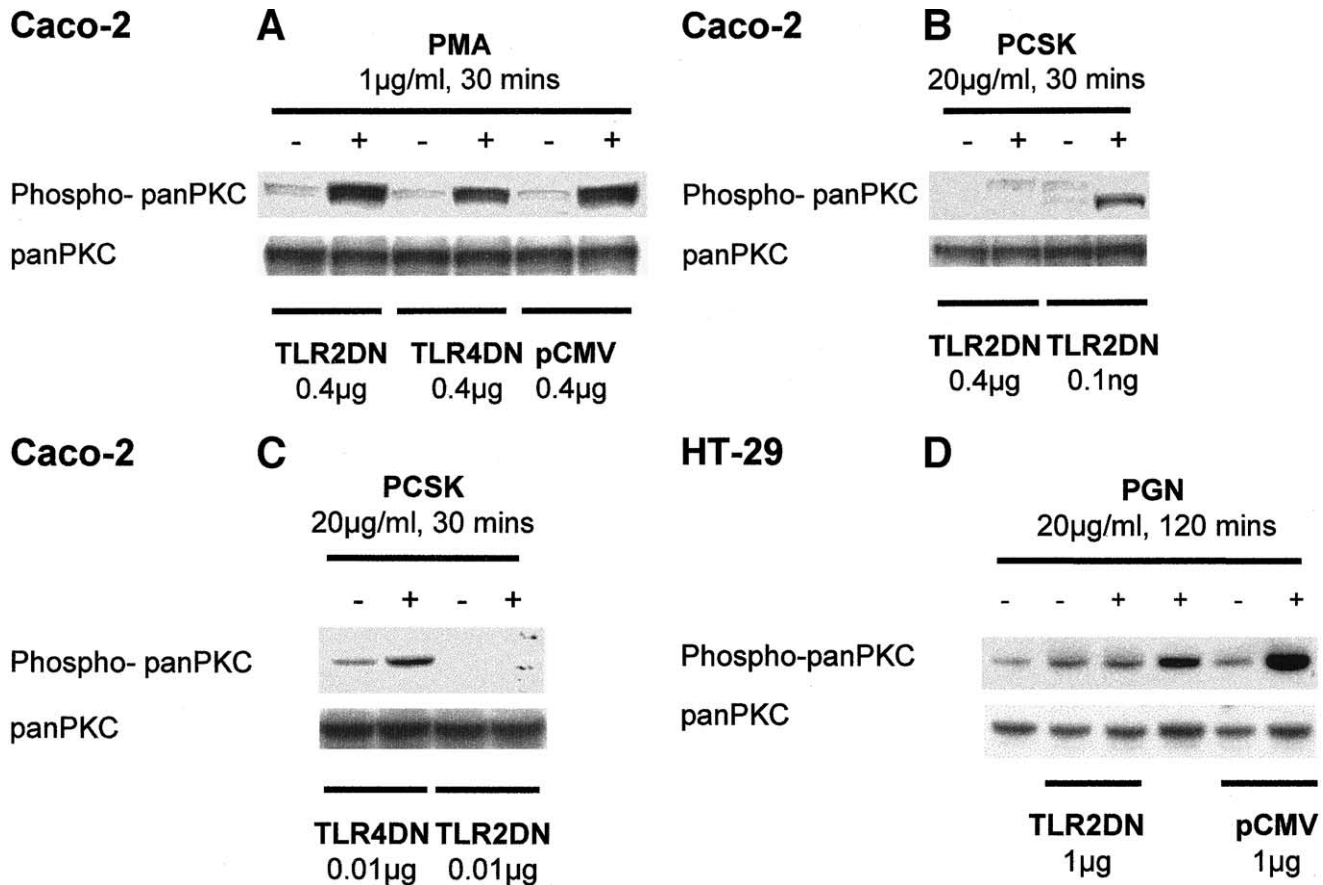


**Figure 5.** TLR2 ligand-induced phosphorylation of PKC complex is blocked specifically by dominant-negative TLR2. (A–C) Caco-2 and (D) HT-29 cell monolayers were transfected transiently with dominant-negative versions of TLR2 (TLR2DN), TLR4 (TLR4DN), or pCMV vector control (0.1 ng–1.0 μg/well), as described in the Materials and Methods section. Two days after transfection, cells were treated with (A) PMA (1 μg/mL, 30 min), (B, C) Pam<sub>3</sub>CysSK4 (20 μg/mL, 30 min), or (D) PGN (20 μg/mL, 120 min), respectively. Cell lysates were immunoblotted and probed with anti-phospho-panPKC antibody, as described in the Materials and Methods section. To exclude alteration of PKC expression owing to transfection and to confirm equal loading, blots were reprobed with anti-panPKC and anti-β-actin (data not shown), respectively.

TLR2 or TLR4. Accordingly, PMA-induced activation of PKC complex neither was prevented nor altered by TLR2DN or TLR4DN when compared with control vector (Figure 5A) or nontransfected cells (Figure 1A), thus excluding nonspecific inhibitory effects caused by transfection. However, Pam<sub>3</sub>CysSK4-induced rapid phosphorylation of PKC complex was blocked significantly in TLR2DN-transfected cells (Figure 5B, 0.4 μg/chamber; Figure 5C, 0.01 μg/chamber). A lesser concentration of only 0.1 ng/chamber of TLR2DN was suboptimal because Pam<sub>3</sub>CysSK4-induced PKC phosphorylation was not inhibited (Figure 5B), suggesting a concentration-dependent mutant-specific effect. In the control experiment, Pam<sub>3</sub>CysSK4-induced phosphorylation of PKC complex was not blocked by TLR4DN (Figure 5C), implying that TLR2 is specifically mediating PKC phosphorylation in response to the TLR2 ligand Pam<sub>3</sub>CysSK4. In addition, PGN-induced activation of PKC was blocked significantly by TLR2DN, but

not by control vector in HT-29 cells (Figure 5D), confirming that PKC activation is a TLR2-specific signaling effect. Kinetics of PKC phosphorylation induced by TLR2 ligands were comparable between nontransfected and control (TLR4DN or pCMV) transfected cells. Transfection did not alter total protein expression of nonphosphorylated PKC (Figure 5A–D).

#### Divergent Downstream Effects Via PKC

Downstream, Pam<sub>3</sub>CysSK4 led to rapid phosphorylation of the PKC-specific endogenous substrate MARCKS after 15 and 30 minutes of stimulation (Figure 6A). PKC activation is known to lead to activation of the transcriptional factor AP-1.<sup>47</sup> However, TLR2 ligands did not induce AP-1-dependent luciferase activity in Caco-2 cells (Figure 6B). In contrast, the phorbol ester PMA (1 μg/mL) induced a 3-fold increase in AP-1-dependent luciferase activity (326% ± 44% control) after 4 hours of stimulation (Figure 6B), which was

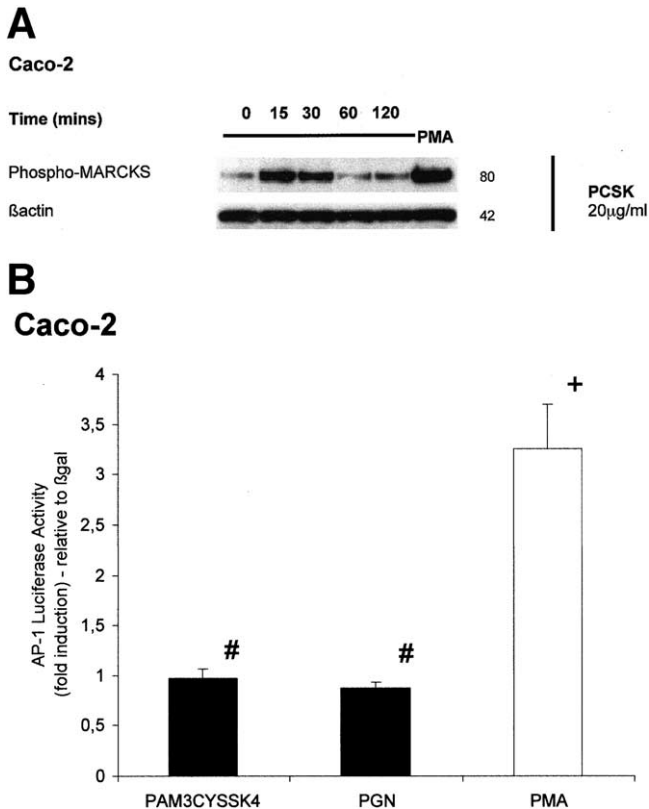


**Figure 6.** TLR2 ligands induce selective downstream effects via PKC substrates. (A) Caco-2 monolayers were treated with Pam<sub>3</sub>CysSK4 (20 μg/mL) for varying time periods (15–120 min) and subjected to immunoblotting with isoform-specific antibody to phosphorylated MARCKS. PMA (1 μg/mL) was used as presumed positive control (30-min stimulation). To confirm equal loading, blots were reprobbed with anti-β-actin. (B) Caco-2 monolayers grown on 6-well plates were cotransfected with pAP1-specific luciferase construct (0.5 μg/well) and pSV-β-galactosidase expression vector (0.1 μg/well). Two days after transfection, confluent cells were stimulated with Pam<sub>3</sub>CysSK4 (10 μg/mL), PGN (10 μg/mL), or PMA (1 μg/mL) for 4 hours. Modulation of AP-1 activity was determined by luciferase assay in cell lysates, normalized to β-galactosidase activity, and compared with negative controls, as described in the Materials and Methods section. Presented data reflect 3 independent experiments, each performed in triplicate per condition. Data are expressed as means ± SD% control. #Pam<sub>3</sub>CysSK4 or PGN vs. negative control,  $P > 0.05$ ; +PMA vs. Pam<sub>3</sub>CysSK4 or PGN,  $P < 0.001$ .

blocked almost completely by pretreating (30 min) the cells with the conventional PKC isoform inhibitor Gö6976 (5 μmol/L<sup>48</sup>; 112% ± 33% control), but only partially with the specific PKCδ inhibitor rottlerin (10 μmol/L<sup>49</sup>; 169% ± 30% control) (data not shown). In contrast to Pam<sub>3</sub>CysSK4, which may be inactivated easily by, for example, oxidation in cell culture media,<sup>44</sup> PMA appears to exhibit a longer half-life, resulting in prolonged or delayed activation of certain PKC isoforms.<sup>50</sup> Thus, these results suggest that biologic differences in kinetics of stimulus-dependent activation of distinct PKC-isoform patterns may lead to contrasting downstream signaling effects in IEC.

## TLR2-Induced PKC Activation Leads to Increase of TER in IECs

PKC activation has been implicated in the regulation of epithelial barrier integrity.<sup>2,51,52</sup> To assess

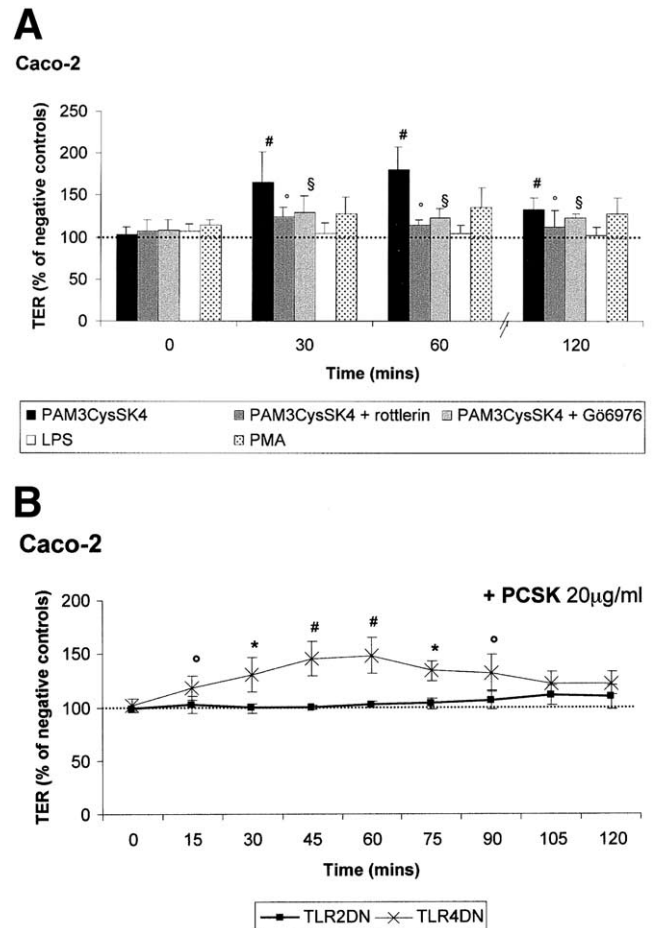


**Figure 7.** (A) The TLR2 ligand Pam<sub>3</sub>CysSK4 increases intestinal TER in a PKC-dependent pathway. Caco-2 grown on inserts was used 21–30 days after seeding. After apical and basolateral stimulation with Pam<sub>3</sub>CysSK4 (20 μg/mL), with or without pretreatment of specific PKC isoform antagonists rottlerin (10 μmol/L) or Gö6976 (5 μmol/L), LPS (1 μg/mL) or PMA (1 μg/mL) TER was measured under standardized conditions over indicated time periods with matched negative controls on each 6-well plate, as described in the Materials and Methods section. Data reflect at least 3 independent experiments per condition; each were performed in triplicate. Data are expressed as means ± SD% control. #Pam<sub>3</sub>CysSK4, 0 vs. 30, 120 min,  $P < 0.05$ ; 0 vs. 60 minutes,  $P < 0.01$ . °Pam<sub>3</sub>CysSK4/rottlerin, 0 vs. 30, 60, 120 min,  $P > 0.17$ . §Pam<sub>3</sub>CysSK4/Gö6976, 0 vs. 30, 60, 120 min,  $P > 0.16$ . ■, PAM<sub>3</sub>CysSK4; ■, PAM<sub>3</sub>CysSK4 + rottlerin; ■, PAM<sub>3</sub>CysSK4 + Gö6976; □, LPS; ▨, PMA. (B) TLR2 ligand-increased transepithelial resistance is blocked specifically by dominant-negative TLR2. Caco-2 monolayers grown on permeable inserts were transfected with dominant-negative versions of TLR2 (TLR2DN) or TLR4 (TLR4DN) (0.4 μg/chamber). After apical and basolateral stimulation with Pam<sub>3</sub>CysSK4 (20 μg/mL), TER was measured under standardized conditions over indicated time periods. Data comprise at least 3 independent experiments per condition, each performed in triplicate with matched negative controls. Data are expressed as means ± SD% control. (TLR4DN- vs. TLR2DN-transfected monolayers: \* $P < 0.01$ ; # $P < 0.001$ ; ° $P < 0.05$ ). ■, TLR2DN; X, TLR4DN.

whether Pam<sub>3</sub>CysSK4-induced PKC activation may affect intestinal epithelial barrier function, Caco-2 cells were grown on inserts and TER was measured in the presence or absence of Pam<sub>3</sub>CysSK4 (20 µg/mL) with or without pretreatment of PKC isoform-selective antagonists. As shown in Figure 7A, stimulation with Pam<sub>3</sub>CysSK4 (20 µg/mL) rapidly led to an almost 2-fold increase of TER after 30 minutes (165% ± 36% control), which peaked after 60 minutes (180% ± 27% control) in parallel with PKC activation (Figures 1 and 2). TER decreased back toward baseline levels after 120 minutes of stimulation (133% ± 14% control) in parallel with PKC inactivation. No further TER changes were observed when followed-up for over 24 hours (data not shown). The Pam<sub>3</sub>CysSK4-induced TER increase was almost completely abolished when cells were pretreated with the PKC inhibitor rottlerin (60 min, 115% ± 6% control) or Gö6976 (60 min, 124% ± 11% control) for 30 minutes, suggesting a role for both conventional and novel PKC isoforms in Pam<sub>3</sub>CysSK4-induced enhancement of intestinal epithelial barrier integrity. In comparison, the PKC activator PMA (1 µg/mL) induced only a 1.4-fold increase of TER (60 min, 135% ± 24% control; 120 min, 128% ± 18% control), which was not significant (0 vs. 60 min,  $P > 0.27$ ; 0 vs. 120 min,  $P > 0.32$ ) and was comparable with recently published results by others.<sup>52</sup> In contrast, the TLR4 ligand LPS, which did not activate PKC complex, also did not affect intestinal epithelial barrier function (60 min, 105% ± 10% control; 0 vs. 60 min,  $P > 0.81$ ) at any time point tested for up to 24 hours (data only shown up to 2 h), implying selective specificity of TER increase in response to TLR2 ligands via PKC.

To confirm that the Pam<sub>3</sub>CysSK4-induced TER increase was mediated via TLR2, Caco-2 cells were transfected with TLR2DN or TLR4DN and TER was assessed after stimulation with Pam<sub>3</sub>CysSK4 (Figure 7B). Monolayers of the transfected cells showed steady-state TER, with comparable baseline readings to age-matched nontransfected epithelia when followed-up for up to 120 hours after transfection (data not shown). In TLR4DN-transfected cells, the Pam<sub>3</sub>CysSK4-induced TER increase reached a maximum of 148% ± 17% compared with nonstimulated TLR4DN-transfected cells after 60 minutes of stimulation, which was not altered significantly compared with that observed in nontransfected epithelia (Pam<sub>3</sub>CysSK4-stimulation, TLR4DN-transfected vs. nontransfected, 0, 30, 60, and 120 min,  $P > 0.08$ ). However, the Pam<sub>3</sub>CysSK4-induced TER increase was abolished completely in TLR2DN-transfected cells, suggesting that this effect specifically requires TLR2.

### TLR2-Induced TER Increase Correlates With ZO-1 Redistribution Via PKC

To assess changes of subcellular distribution of TJ-associated proteins that may occur during TLR2-induced increase of TER, confocal microscopy of highly differentiated Caco-2 monolayers was performed after exposure to Pam<sub>3</sub>CysSK4 (20 µg/mL, 60 min). After stimulation, membrane-associated ZO-1 redistributed to further apical TJ areas forming distinct and consolidated lateral cell-cell contacts in comparison with same-depth negative controls (85–90 µm) analyzed by (X/Y)-Z-section confocal immunofluorescence (Figure 8A). Alteration of ZO-1 distribution was confirmed in all images examined and correlated in a timely manner with Pam<sub>3</sub>CysSK4-induced TER increase. When pretreating monolayers with PKC inhibitors (Gö6976 and rottlerin) for 30 minutes, Pam<sub>3</sub>CysSK4-induced alteration of ZO-1 distribution was blocked significantly after 60 minutes of stimulation (Figure 8B), correlating with inhibition of TER increase via PKC (Figure 6). In contrast, stimulation with Pam<sub>3</sub>CysSK4 did not induce any evident TJ-associated morphologic changes of occludin or claudin-1 (Figure 8A). Pam<sub>3</sub>CysSK4 also did not affect organization of the actin cytoskeleton. In contrast, PMA (1 µg/mL, 60 min) induced disruption of ZO-1 (Figure 9), which correlated with a lack of significant TER increase.

### Discussion

The present study provides evidence that PKC functionally participates in the mammalian TLR2 signaling pathway in IECs. Our results show that TLR2 ligands lead to concentration- and time-dependent activation (i.e., phosphorylation, translocation, and increase of enzymatic activity) of at least 2 PKC-specific isoforms in IECs: conventional PKC $\alpha$  and novel PKC $\delta$ . In 2 different human IEC lines, activation of these kinases after stimulation with TLR2 ligands was maximal at 15–30 minutes for phosphorylation and at 60 minutes for translocation, consistent with observations in other cell lines in response to the TLR4 ligand LPS.<sup>23,53,54</sup> However, in contrast, our results also suggest that PKC activation is not involved in TLR4 signaling in IECs, implying ligand-dependent TLRx-specific features of signaling via distinct PKC isoforms in different cell types. Phosphorylation of PKC complex was blocked completely by transfection with a TLR2 deletion mutant, but not with a TLR4 deletion mutant, confirming that TLR2-ligand-stimulated activation of PKC is mediated specifically through TLR2 in IECs.

Based on the observation that TLR2 ligands induce neither nuclear factor  $\kappa$  B activation nor interleukin 8

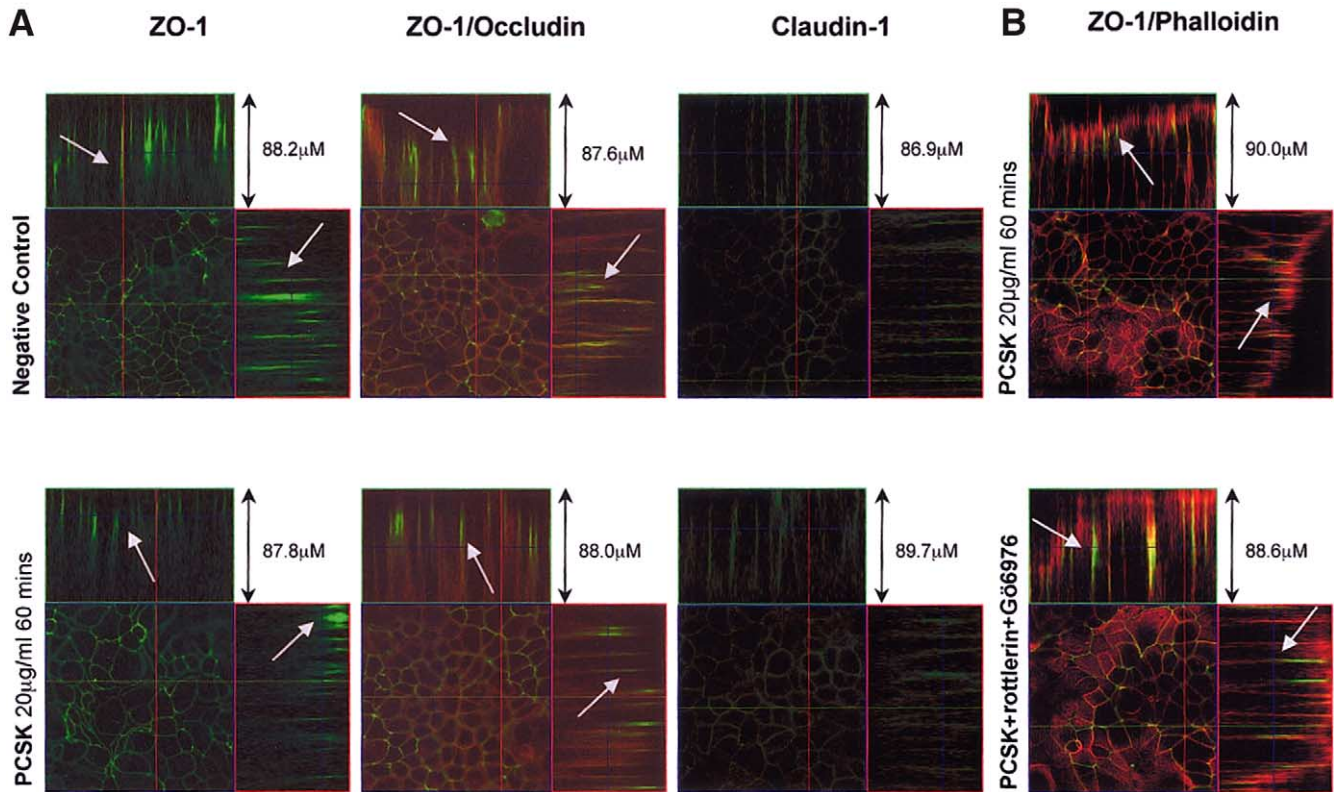


**Figure 8.** TLR2 ligand-induced increase of transepithelial resistance correlates with apical redistribution and tightening of ZO-1 in a PKC-dependent manner. (A, B) Caco-2 cells grown on chamber slides until differentiated were treated with Pam<sub>3</sub>CysSK4 (20 µg/mL) for 60 minutes (B) with or (A) without pretreatment of specific PKC-isoform antagonists, rottlerin (10 µmol/L) and Gö6976 (5 µmol/L) for 30 minutes, and TJ assembly was assessed by specific antibodies to (A, B) ZO-1, (A) claudin-1, or (A) occludin followed by FITC- (ZO-1; claudin-1)/CY5- (occludin) conjugated secondary antibody and confocal microscopy, as described in the Materials and Methods section. Representative images of XZ-, YZ-, and XY-stacks are shown. Red and green lines indicate location of XZ/YZ-stacks in XY-stack, blue lines indicate location of XY-stack in XZ/YZ-stacks, respectively. (B) Cells were counterstained with phalloidin-rhodamine to outline cell boundaries. White arrow indicates localization of ZO-1. (63×/1.4, oil, zoom 1.0, total scanning depth of 30 Z-stacks per monolayer is indicated per individual image.)

secretion in some IEC lines, it recently has been suggested that IECs are broadly hypo-responsive to TLR2 ligands.<sup>16</sup> AP-1 is an abundantly expressed transcription factor that is central to several immune and inflammatory responses mediated via PKC.<sup>47</sup> In this study, we show that TLR2-induced PKC activation did not stimulate AP-1 transcriptional activity in IECs. Instead, we provide evidence that TLR2 may stimulate other, previously unappreciated, functional responses via PKC.

PKC has been implicated in the regulation of intestinal epithelial integrity.<sup>2,51,52</sup> Ligand-specific activation of distinct patterns of PKC isoforms can exert paradoxical effects in intestinal epithelial monolayers: either increasing or decreasing intestinal permeability.<sup>2,48,52,55–57</sup> In this study, Pam<sub>3</sub>CysSK4 treatment led to a time-dependent increase in TER via TLR2, which correlated with PKCα/δ activation. The TER increase was significantly abolished when pretreating monolayers with the specific PKC isoform inhibitors: rottlerin (a specific antagonist for PKCδ in the concentrations used here<sup>58</sup>) and Gö6976

(a selective inhibitor of the conventional PKC subfamily [PKCα, β, γ]<sup>59</sup>), suggesting that TLR2-induced activation of conventional and novel PKC isoforms increases TER. Loss of TLR2 function did not induce impaired barrier function in nonstimulated intestinal epithelial monolayers, as shown by steady-state TER readings comparable with those in nontransfected monolayers constitutively expressing TLR2.

Little is known about the processes modulating distinct TJ assembly when TER increases in IECs. Standardized confocal analysis by uniform Z sections to describe morphologic changes of intestinal epithelial TJ contacts mostly is used in studies when evaluating TER decreases rather than increases. Activation of certain PKC isoforms may involve the release of calcium stores, which is critical for TJ formation and tightness.<sup>51,60</sup> PKC isoforms specifically may regulate the sorting and assembly of ZO-1, preserving proper development of TJs and leading to an increase of TER.<sup>2,61</sup> This study showed that stimulation with the TLR2 ligand Pam<sub>3</sub>CysSK4 results

## ZO-1

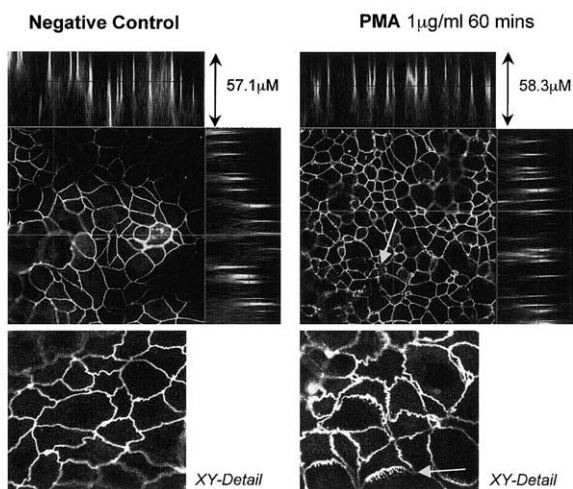


**Figure 9.** PMA-induced disruption of ZO-1 correlates with lack of TER increase. Caco-2 cells grown on chamber slides were treated with PMA (1  $\mu\text{g}/\text{mL}$ , 60 min) or left untreated and ZO-1 was assessed by staining with a specific antibody followed by FITC-conjugated secondary antibody and confocal microscopy, as described in the Materials and Methods section. Cells were counterstained with phalloidin to outline cell boundaries (data not shown). Representative images of XZ-, YZ-, and XY-stacks are shown (monochannel: FITC). *White arrow* indicates disruption of ZO-1 in response to PMA stimulation. ( $63\times/1.4$ , oil, zoom 1.0, total scanning depth of 30 Z-stacks per monolayer is indicated per individual image.)

in apical tightening of ZO-1, which correlated with activation of PKC $\alpha/\delta$  and PKC-mediated TER increase via TLR2 in Caco-2 cells. Of note, a similar morphologic effect on ZO-1 distribution so far has not been described in response to other PKC activators in IECs. Pam<sub>3</sub>CysSK4-induced translocation of ZO-1 was prevented by pretreatment with selective PKC inhibitors that correlated with the inhibition of Pam<sub>3</sub>CysSK4-induced TER increase. This finding suggests that TLR2-induced activation of distinct PKC-specific isoforms leads to a sealing pattern of apical ZO-1, resulting in an increase in TJ-associated barrier integrity. It is possible that TLR2 ligand-induced ZO-1 translocation could trigger the tightening of other interconnecting TJ contacts between adjacent epithelial cells resulting in increased TER. It recently has been suggested that barrier function may be augmented by enhancing the TJ complex via recruitment<sup>49</sup> and up-regulation<sup>62</sup> of claudin-1. However, any other Pam<sub>3</sub>CysSK4-induced TJ alterations must be subtle, because no changes in distribution of 2 major TJ proteins, claudin-1 and occludin, were detectable.

Moreover, reorganization of the actin cytoskeleton, which also may be regulated by specific PKC isoforms,<sup>51</sup> was absent. However, we found that Pam<sub>3</sub>CysSK4 led to phosphorylation of MARCKS, one of the major cellular

targets of PKC isoforms. It recently has been shown that MARCKS also serves as an actin cross-linking protein,<sup>63</sup> potentially participating in modulation of epithelial integrity. ZO-1 also may bind components of the TJ complex to the actin cytoskeleton.<sup>64</sup> It is possible that TLR2-induced intestinal epithelial barrier enhancement results from potential convergence of various signaling interactions and pathways downstream of PKC, which may interact by bridging to the actin cytoskeleton.

Because the most prominent intracellular targets of diacylglycerol and of the functionally analogous phorbol esters belong to the PKC family,<sup>65</sup> PMA has been used as presumed positive control of broad PKC isoform activation in this study, although the current knowledge regarding patterns and effects of PMA-induced PKC isoform activation is limited in IECs. In contrast to TLR2 ligands, PMA-induced phosphorylation of PKC complex used other PKC isoforms with different kinetics. It is already well known that differences between PKC isoforms for their ligand and substrate specificity may lead to different physiologic responses in individual cell types.<sup>66</sup> Consequently, PMA-induced selective activation of PKC complex led to downstream effects that were distinct from those seen after treatment with TLR2 ligands (e.g., AP-1 activation). It recently has been shown that intestinal epithelial monolayer disassembly in response to prolonged exposure to PMA correlates with PKC-associated alterations in the perijunctional ring of actin and myosin,<sup>55</sup> which may have accounted for our observation of disruption of ZO-1 correlating with a lack of TER increase. There also is emerging evidence that several cellular processes induced by PMA may depend on non-PKC-triggered targets, disproving the notion that all phorbol-ester effects must be mediated solely by PKC isozymes.<sup>65,67</sup> PMA-specific induction of different PKC- as well as non-PKC-associated signaling events may have contributed significantly to these contrasting downstream effects when compared with TLR2 ligands in IECs.

Taken together, our data suggest that a specific physiologic consequence of the increase in certain PKC isozyme activation by TLR2 is enhancement of intestinal epithelial barrier function, which correlates with distinct TJ-associated morphologic changes. Further studies are needed to clarify in detail the TLR2-triggered Ca<sup>2+</sup> pathways that may regulate the complex TJ-associated interactions of membrane signaling partners leading to enhancement of barrier integrity. It will be important to determine whether PKC isoforms are central downstream components of both the TIRAP/Mal- and MyD88-dependent signaling pathways via TLR2.<sup>68,69</sup> Because PKC

is known to comprise a large family of enzymes, additional isoforms may be involved in TLR2-induced phosphorylation of PKC complex. More importantly, parallel or subsequent activation of opposing PKC isoforms may cause differential downstream effects in epithelial cells.<sup>48,51,70</sup> In this context, further studies are required to identify whether other TLRx ligands activate different PKC isoforms, cooperatively or competitively increasing or decreasing intestinal epithelial barrier permeability. It is possible that bacterial ligands may counterbalance each other via TLRs, maintaining barrier homeostasis of the normal intestinal epithelium. It remains to be determined whether pathogenic bacteria-induced decreases in TER also may be mediated via TLRx.

Our results suggest that impaired function of TLR2 itself does not lead to increased intestinal epithelial permeability *in vitro*. In this context, it will be essential to show whether lack of host-protective TLR2 ligands in the lumen that may be present in the resident microflora could lead to loss of barrier protection, facilitating invasion of pathogenic bacteria in disease. It recently has been shown that probiotics, which may help some patients with inflammatory bowel disease,<sup>71</sup> enhance intestinal epithelial barrier function.<sup>6</sup> Although the underlying mechanisms remain to be determined, it is possible that certain probiotic compounds may contain TLR2-specific immunostimulatory features, leading to amelioration of colitis by restoring intestinal epithelial barrier integrity. Specific targeting of TLR2 possibly could help in the design of novel adjuvant therapeutic means to enhance intestinal epithelial barrier function to protect the underlying host.

In conclusion, the present study describes the induction of a novel innate immune pathway through certain PKC isoforms by distinct bacterial ligands, critically regulating intestinal epithelial barrier function by selective rearrangement of TJ-associated ZO-1 via a specific mechanism dependent from TLR2 signaling. Further studies are needed to investigate whether imbalance of the resident microflora may lead to barrier dysfunction induced by TJ disassembly through TLRx-PKC isozyme dysregulation.

## References

- Mitic LL, Van Itallie CM, Anderson JM. Molecular physiology and pathophysiology of tight junctions I. Tight junction structure and function: lessons from mutant animals and proteins. *Am J Physiol* 2000;279:G250–G254.
- Stuart RO, Nigam SK. Regulated assembly of tight junctions by protein kinase C. *Proc Natl Acad Sci U S A* 1995;92:6072–6076.
- Berkes J, Viswanathan VK, Savkovic SD, Hecht G. Intestinal epithelial responses to enteric pathogens: effects on the tight junction barrier, ion transport, and inflammation. *Gut* 2003;52:439–451.
- Kindon H, Pothoulakis C, Thim L, Lynch-Devaney K, Podolsky DK. Trefoil peptide protection of intestinal epithelial barrier function: cooperative interaction with mucin glycoprotein. *Gastroenterology* 1995;109:516–523.
- Czerucka D, Dahan S, Mograbi B, Rossi B, Rampal P. *Saccharomyces boulardii* preserves the barrier function and modulates the signal transduction pathway induced in enteropathogenic *Escherichia coli*-infected T84 cells. *Infect Immun* 2000;68:5998–6004.
- Madsen K, Cornish A, Soper P, McKaigney C, Jijon H, Yachimec C, Doyle J, Jewell L, De Simone C. Probiotic bacteria enhance murine and human intestinal epithelial barrier function. *Gastroenterology* 2001;121:580–591.
- Janeway CA Jr, Medzhitov R. Innate immune recognition. *Annu Rev Immunol* 2002;20:197–216.
- Cario E, Rosenberg IM, Brandwein SL, Beck PL, Reinecker HC, Podolsky DK. Lipopolysaccharide activates distinct signaling pathways in intestinal epithelial cell lines expressing Toll-like receptors. *J Immunol* 2000;164:966–972.
- Cario E, Podolsky DK. Differential alteration in intestinal epithelial cell expression of toll-like receptor 3 (TLR3) and TLR4 in inflammatory bowel disease. *Infect Immun* 2000;68:7010–7017.
- Gewirtz AT, Navas TA, Lyons S, Godowski PJ, Madara JL. Cutting edge: bacterial flagellin activates basolaterally expressed TLR5 to induce epithelial proinflammatory gene expression. *J Immunol* 2001;167:1882–1885.
- Abreu MT, Vora P, Faure E, Thomas LS, Arnold ET, Arditi M. Decreased expression of Toll-like receptor-4 and MD-2 correlates with intestinal epithelial cell protection against dysregulated proinflammatory gene expression in response to bacterial lipopolysaccharide. *J Immunol* 2001;167:1609–1616.
- Fusunyan RD, Nanthakumar NN, Baldeon ME, Walker WA. Evidence for an innate immune response in the immature human intestine: toll-like receptors on fetal enterocytes. *Pediatr Res* 2001;49:589–593.
- Haller D, Russo MP, Sartor RB, Jobin C. IKK beta and phosphatidylinositol 3-kinase/Akt participate in non-pathogenic gram-negative enteric bacteria-induced RelA phosphorylation and NF-kappa B activation in both primary and intestinal epithelial cell lines. *J Biol Chem* 2002;277:38168–38178.
- Cario E, Brown D, McKee M, Lynch-Devaney K, Gerken G, Podolsky DK. Commensal-associated molecular patterns induce selective toll-like receptor-trafficking from apical membrane to cytoplasmic compartments in polarized intestinal epithelium. *Am J Pathol* 2002;160:165–173.
- Cario E. Toll-like receptors and gastrointestinal disease: from bench to bedside? *Curr Opin Gastroenterol* 2002;18:696–704.
- Melmed G, Thomas LS, Lee N, Tesfay SY, Lukasek K, Michelsen KS, Zhou Y, Hu B, Arditi M, Abreu MT. Human intestinal epithelial cells are broadly unresponsive to Toll-like receptor 2-dependent bacterial ligands: implications for host-microbial interactions in the gut. *J Immunol* 2003;170:1406–1415.
- Otte JM, Cario E, Podolsky DK. Mechanisms of cross-hypo-responsiveness to Toll-like receptor ligands in intestinal epithelial cells. *Gastroenterology* 2004;126:1054–1070.
- Suzuki M, Hisamatsu T, Podolsky DK. Gamma interferon augments the intracellular pathway for lipopolysaccharide (LPS) recognition in human intestinal epithelial cells through coordinated up-regulation of LPS uptake and expression of the intracellular Toll-like receptor 4-MD-2 complex. *Infect Immun* 2003;71:3503–3511.
- Abreu MT, Arnold ET, Thomas LS, Gonsky R, Zhou Y, Hu B, Arditi M. TLR4 and MD-2 expression is regulated by immune-mediated signals in human intestinal epithelial cells. *J Biol Chem* 2002;277:20431–20437.
- Newton AC. Protein kinase C: structure, function, and regulation. *J Biol Chem* 1995;270:28495–28498.

21. Dekker LV, Parker PJ. Protein kinase C—a question of specificity. *Trends Biochem Sci* 1994;19:73–77.
22. Avila A, Silverman N, Diaz-Meco MT, Moscat J. The Drosophila atypical protein kinase C-ref(2)p complex constitutes a conserved module for signaling in the toll pathway. *Mol Cell Biol* 2002;22:8787–8795.
23. Aksoy E, Amraoui Z, Gorieli S, Goldman M, Willems F. Critical role of protein kinase C epsilon for lipopolysaccharide-induced IL-12 synthesis in monocyte-derived dendritic cells. *Eur J Immunol* 2002;32:3040–3049.
24. Rhee SH, Jones BW, Toshchakov V, Vogel SN, Fenton MJ. Toll-like receptors 2 and 4 activate STAT1 serine phosphorylation by distinct mechanisms in macrophages. *J Biol Chem* 2003;278:22506–22512.
25. Castrillo A, Pennington DJ, Otto F, Parker PJ, Owen MJ, Bosca L. Protein kinase C epsilon is required for macrophage activation and defense against bacterial infection. *J Exp Med* 2001;194:1231–1242.
26. Franchi-Gazzola R, Visigalli R, Bussolati O, Gazzola GC. Involvement of protein kinase C epsilon in the stimulation of anionic amino acid transport in cultured human fibroblasts. *J Biol Chem* 1996;271:26124–26130.
27. Deszo EL, Brake DK, Cengel KA, Kelley KW, Freund GG. CD45 negatively regulates monocytic cell differentiation by inhibiting phorbol 12-myristate 13-acetate-dependent activation and tyrosine phosphorylation of protein kinase C delta. *J Biol Chem* 2001;276:10212–10217.
28. Fantini J, Verrier B, Marvaldi J, Mauchamp J. In vitro differentiated HT 29-D4 clonal cell line generates leakproof and electrically active monolayers when cultured in porous-bottom culture dishes. *Biol Cell* 1989;65:163–169.
29. Peterson MD, Mooseker MS. An in vitro model for the analysis of intestinal brush border assembly. I. Ultrastructural analysis of cell contact-induced brush border assembly in Caco-2BBE cells. *J Cell Sci* 1993;105:445–460.
30. Peterson MD, Bement WM, Mooseker MS. An in vitro model for the analysis of intestinal brush border assembly. II. Changes in expression and localization of brush border proteins during cell contact-induced brush border assembly in Caco-2BBE cells. *J Cell Sci* 1993;105:461–472.
31. Xu Y, Tao X, Shen B, Horng T, Medzhitov R, Manley JL, Tong L. Structural basis for signal transduction by the Toll/interleukin-1 receptor domains. *Nature* 2000;408:111–115.
32. Smith MF Jr, Mitchell A, Li G, Ding S, Fitzmaurice AM, Ryan K, Crowe S, Goldberg JB. Toll-like receptor (TLR) 2 and TLR5, but not TLR4, are required for Helicobacter pylori-induced NF-kappa B activation and chemokine expression by epithelial cells. *J Biol Chem* 2003;278:32552–32560.
33. Faure E, Equils O, Sieling PA, Thomas L, Zhang FX, Kirschning CJ, Polentarutti N, Muzio M, Arditi M. Bacterial lipopolysaccharide activates NF-kappaB through toll-like receptor 4 (TLR-4) in cultured human dermal endothelial cells. Differential expression of TLR-4 and TLR-2 in endothelial cells. *J Biol Chem* 2000;275:11058–11063.
34. Bulut Y, Faure E, Thomas L, Karahashi H, Michelsen KS, Equils O, Morrison SG, Morrison RP, Arditi M. Chlamydial heat shock protein 60 activates macrophages and endothelial cells through Toll-like receptor 4 and MD2 in a MyD88-dependent pathway. *J Immunol* 2002;168:1435–1440.
35. Ahn JD, Morishita R, Kaneda Y, Lee SJ, Kwon KY, Choi SY, Lee KU, Park JY, Moon IJ, Park JG, Yoshizumi M, Ouchi Y, Lee IK. Inhibitory effects of novel AP-1 decoy oligodeoxynucleotides on vascular smooth muscle cell proliferation in vitro and neointimal formation in vivo. *Circ Res* 2002;90:1325–1332.
36. Heinz S, Haehnel V, Karaghiosoff M, Schwarzfischer L, Muller M, Krause SW, Rehli M. Species-specific regulation of Toll-like receptor 3 genes in men and mice. *J Biol Chem* 2003;278:21502–21509.
37. Knight A, Carvajal J, Schneider H, Coutelle C, Chamberlain S, Fairweather N. Non-viral neuronal gene delivery mediated by the HC fragment of tetanus toxin. *Eur J Biochem* 1999;259:762–769.
38. Sabroe I, Prince LR, Jones EC, Horsburgh MJ, Foster SJ, Vogel SN, Dower SK, Whyte MK. Selective roles for Toll-like receptor (TLR)2 and TLR4 in the regulation of neutrophil activation and life span. *J Immunol* 2003;170:5268–5275.
39. Hirschfeld M, Ma Y, Weis JH, Vogel SN, Weis JJ. Cutting edge: repurification of lipopolysaccharide eliminates signaling through both human and murine toll-like receptor 2. *J Immunol* 2000;165:618–622.
40. Iwaki D, Mitsuzawa H, Murakami S, Sano H, Konishi M, Akino T, Kuroki Y. The extracellular toll-like receptor 2 domain directly binds peptidoglycan derived from Staphylococcus aureus. *J Biol Chem* 2002;277:24315–24320.
41. Inohara N, Ogura Y, Fontalba A, Gutierrez O, Pons F, Crespo J, Fukase K, Inamura S, Kusumoto S, Hashimoto M, Foster SJ, Moran AP, Fernandez-Luna JL, Nunez G. Host recognition of bacterial muramyl dipeptide mediated through NOD2. Implications for Crohn's disease. *J Biol Chem* 2003;278:5509–5512.
42. Girardin SE, Boneca IG, Viala J, Chamillard M, Labigne A, Thomas G, Philpott DJ, Sansonetti PJ. Nod2 is a general sensor of peptidoglycan through muramyl dipeptide (MDP) detection. *J Biol Chem* 2003;278:8869–8872.
43. Hisamatsu T, Suzuki M, Reinecker HC, Nadeau WJ, McCormick BA, Podolsky DK. CARD15/NOD2 functions as an antibacterial factor in human intestinal epithelial cells. *Gastroenterology* 2003;124:993–1000.
44. Morr M, Takeuchi O, Akira S, Simon MM, Muhlradt PF. Differential recognition of structural details of bacterial lipopeptides by toll-like receptors. *Eur J Immunol* 2002;32:3337–3347.
45. Shirai Y, Saito N. Activation mechanisms of protein kinase C: maturation, catalytic activation, and targeting. *J Biochem (Tokyo)* 2002;132:663–668.
46. Li C, Wang Y, Gao L, Zhang J, Shao J, Wang S, Feng W, Wang X, Li M, Chang Z. Expression of toll-like receptors 2 and 4 and CD14 during differentiation of HL-60 cells induced by phorbol 12-myristate 13-acetate and 1 alpha, 25-dihydroxy-vitamin D(3). *Cell Growth Differ* 2002;13:27–38.
47. Ways DK, Qin W, Garris TO, Chen J, Hao E, Cooper DR, Usala SJ, Parker PJ, Cook PP. Effects of chronic phorbol ester treatment on protein kinase C activity, content, and gene expression in the human monoblastoid U937 cell. *Cell Growth Differ* 1994;5:161–169.
48. Song JC, Rangachari PK, Matthews JB. Opposing effects of PK-Calpha and PKCepsilon on basolateral membrane dynamics in intestinal epithelia. *Am J Physiol* 2002;283:C1548–C1556.
49. Yoo J, Nichols A, Song JC, Mammen J, Calvo I, Worrell RT, Cuppoletti J, Matlin K, Matthews JB. Bryostatins-1 attenuates TNF-induced epithelial barrier dysfunction: role of novel PKC isozymes. *Am J Physiol* 2003;284:G703–G712.
50. Ahmed S, Kozma R, Lee J, Monfries C, Harden N, Lim L. The cysteine-rich domain of human proteins, neuronal chimerin, protein kinase C and diacylglycerol kinase binds zinc. Evidence for the involvement of a zinc-dependent structure in phorbol ester binding. *Biochem J* 1991;280:233–241.
51. Balda MS, Gonzalez-Mariscal L, Matter K, Cerejido M, Anderson JM. Assembly of the tight junction: the role of diacylglycerol. *J Cell Biol* 1993;123:293–302.
52. Turner JR, Angle JM, Black ED, Joyal JL, Sacks DB, Madara JL. PKC-dependent regulation of transepithelial resistance: roles of MLC and MLC kinase. *Am J Physiol* 1999;277:C554–C562.
53. Hsu YW, Chi KH, Huang WC, Lin WW. Ceramide inhibits lipopolysaccharide-mediated nitric oxide synthase and cyclooxygen-

- ase-2 induction in macrophages: effects on protein kinases and transcription factors. *J Immunol* 2001;166:5388–5397.
54. Kontny E, Kurowska M, Szczepanska K, Maslinski W, Rottlerin, a PKC isozyme-selective inhibitor, affects signaling events and cytokine production in human monocytes. *J Leukoc Biol* 2000;67:249–258.
  55. Hecht G, Robinson B, Koutsouris A. Reversible disassembly of an intestinal epithelial monolayer by prolonged exposure to phorbol ester. *Am J Physiol* 1994;266:G214–G221.
  56. Mullin JM, Laughlin KV, Ginanni N, Marano CW, Clarke HM, Peralta Soler A. Increased tight junction permeability can result from protein kinase C activation/translocation and act as a tumor promotional event in epithelial cancers. *Ann N Y Acad Sci* 2000;915:231–236.
  57. Song JC, Hanson CM, Tsai V, Farokhzad OC, Lotz M, Matthews JB. Regulation of epithelial transport and barrier function by distinct protein kinase C isoforms. *Am J Physiol* 2001;281:C649–C661.
  58. Gschwendt M, Muller HJ, Kielbassa K, Zang R, Kittstein W, Rincke G, Marks F, Rottlerin, a novel protein kinase inhibitor. *Biochem Biophys Res Commun* 1994;199:93–98.
  59. Mukherjee JJ, Chung T, Ways DK, Kiss Z. Protein kinase C $\alpha$  is a major mediator of the stimulatory effect of phorbol ester on phospholipase D-mediated hydrolysis of phosphatidylethanolamine. *J Biol Chem* 1996;271:28912–28917.
  60. Tai YH, Flick J, Levine SA, Madara JL, Sharp GW, Donowitz M. Regulation of tight junction resistance in T84 monolayers by elevation in intracellular Ca<sup>2+</sup>: a protein kinase C effect. *J Membr Biol* 1996;149:71–79.
  61. Balda MS, Gonzalez-Mariscal L, Contreras RG, Macias-Silva M, Torres-Marquez ME, Garcia-Sainz JA, Cereijido M. Assembly and sealing of tight junctions: possible participation of G-proteins, phospholipase C, protein kinase C and calmodulin. *J Membr Biol* 1991;122:193–202.
  62. Kinugasa T, Sakaguchi T, Gu X, Reinecker HC. Claudins regulate the intestinal barrier in response to immune mediators. *Gastroenterology* 2000;118:1001–1011.
  63. Hartwig JH, Thelen M, Rosen A, Janmey PA, Nairn AC, Aderem A. MARCKS is an actin filament crosslinking protein regulated by protein kinase C and calcium-calmodulin. *Nature* 1992;356:618–622.
  64. Fanning AS, Jameson BJ, Jesaitis LA, Anderson JM. The tight junction protein ZO-1 establishes a link between the transmembrane protein occludin and the actin cytoskeleton. *J Biol Chem* 1998;273:29745–29753.
  65. Brose N, Rosenmund C. Move over protein kinase C, you've got company: alternative cellular effectors of diacylglycerol and phorbol esters. *J Cell Sci* 2002;115:4399–4411.
  66. Nakashima S. Protein kinase C $\alpha$  (PKC $\alpha$ ): regulation and biological function. *J Biochem (Tokyo)* 2002;132:669–675.
  67. Kazanietz MG. Novel "nonkinase" phorbol ester receptors: the C1 domain connection. *Mol Pharmacol* 2002;61:759–767.
  68. Fitzgerald KA, Palsson-McDermott EM, Bowie AG, Jefferies CA, Mansell AS, Brady G, Brint E, Dunne A, Gray P, Harte MT, McMurray D, Smith DE, Sims JE, Bird TA, O'Neill LA. Mal (MyD88-adaptor-like) is required for Toll-like receptor-4 signal transduction. *Nature* 2001;413:78–83.
  69. Horng T, Barton GM, Medzhitov R. TIRAP: an adapter molecule in the Toll signaling pathway. *Nat Immunol* 2001;2:835–841.
  70. Chen ML, Pothoulakis C, LaMont JT. Protein kinase C signaling regulates ZO-1 translocation and increased paracellular flux of T84 colonocytes exposed to *Clostridium difficile* toxin A. *J Biol Chem* 2002;277:4247–4254.
  71. Podolsky DK. Inflammatory bowel disease. *N Engl J Med* 2002;347:417–429.

---

Received August 21, 2003. Accepted April 8, 2004.

Address requests for reprints to: Elke Cario, M.D., Division of Gastroenterology and Hepatology, University Hospital of Essen, Institutsgruppe I, Virchowstrasse 171, D-45147 Essen, Germany. e-mail: elke.cario@uni-essen.de; fax: (49) 211-495-7035.

Supported by grants from the Deutsche Forschungsgemeinschaft (Ca226/4-1, Ca226/5-1, Priority Program Innate Immunity), and the Medical Faculty (IFORES) at the University of Essen (to E.C.), and by grants from the National Institutes of Health (DK60049; DK43351) (to D.K.P.).

The authors thank Tularik Inc. (South San Francisco, CA) for kindly providing the dominant-negative constructs of TLR2 and TLR4 through Dr. Carsten J. Kirschning (Institute of Medical Microbiology, Immunology, and Hygiene, Technical University of Munich, Munich, Germany). The authors also thank Dr. Jens Nürnberger (Division of Nephrology, University Hospital of Essen, Essen, Germany) for the gift of the CY5-conjugated goat anti-rabbit antibody.